Experimental Demonstration of a Digital-Twin-Based Risk Map for Proactive Management of Fiber Flapping in a Mesh Network

Chenyu Sun[1,2,3,*], Yilong Chen[3,4], Photios A. Stavrou[2], Yvan Pointurier[3], Gabriel Charlet[3]

[1] Sorbonne University, Paris, France
[2] EURECOM, Sophia-Antipolis, France, * chenyu.sun@eurecom.fr
[3] Huawei Technologies France, Boulogne-Billancourt, France
[4] Université Paris-Saclay, Gif-sur-Yvette, France

Abstract *We experimentally demonstrate a digital-twin-based framework simulates "what-if" fiber flapping and power dips across a mesh optical network, generates risk maps, and recommends proactive adjustments of inline amplifier gain or booster launch power profile to pre-compensate potential degradations, enhancing end-to-end SNR margin and network resilience.*

Introduction

In real-world networks, common short-term intermittent link events (such as fiber flapping, short-term attenuation/flickering, and sudden power dips [1][2]) can trigger burst bit errors and service switching within a millisecond time scale. Engineering practices have shown that these transient events are often difficult to capture and locate using traditional, slower monitoring methods, leading to prolonged troubleshooting cycles and a tendency to fall into reactive repair. Moreover, flapping is often considered a precursor to more severe outages, and early detection and intervention can shift the operation and maintenance from "reactive repair" to "proactive maintenance [3]."

In recent years, network digital twins (DTs) have been defined as virtual representations of real networks, enabling analysis, diagnosis, simulation, and control of real network behaviors through data, models, interfaces, and mapping, with an emphasis on the interaction and mapping between the virtual and real worlds to support closed-loop automation [4]-[9]. For optical networks, both industry and academia have proposed deployment architectures and various DT applications for optical networks, including performance evaluation and optimization [10], fault localization/simulation [11], and more.

A risk map is an action-oriented representation that quantifies the sensitivity of network-wide QoT margins to localize perturbations across network elements, while explicitly preserving the operational constraints of in-service traffic. For events such as short-term flapping or power dips, the network side typically still relies on a reactive "alarm—localization—recovery" process, lacking a systematic mechanism to model event families and incorporate a "risk map + proactive compensation actions" approach to address issues before changes and maintenance activities occur.

This paper proposes and experimentally validates an active framework based on DTs: on a mesh optical network, the DT performs "what-if" simulations of fiber flapping and power dips scenarios, generating a risk map covering optical multiplex sections (OMSs), spans, and services, and recommends proactive adjustments to amplifier gain or booster launch power profile to counteract potential signal-to-noise ratio (SNR) degradation before the events occur. We experimentally demonstrate that the proposed framework can anticipate and mitigate degradation scenarios, improving the span input loss margin under fiber flapping by up to 2.6dB.

Principles

Fig. 1 illustrates how a localized soft failure, such as fiber flapping or transient power dips—initiates impairment propagation across a mesh optical network through coupled physical-layer effects. When a disturbance occurs on a given span, it perturbs the optical power distribution, which in turn excites nonlinear interactions including stimulated Raman scattering (SRS) and spectrum hole burning (SHB) within optical amplifiers. SHB can arise as variations in total input power drive gain compression in the erbium-doped fiber amplifier (EDFA). This leads to wavelength-dependent gain depletion and localized distortions in the gain spectrum. Together with SRS-induced interchannel power transfer, these effects lead to spectral tilt and power redistribution across wavelengths [12][13]. In a mesh optical network, power disturbances continuously propagate and

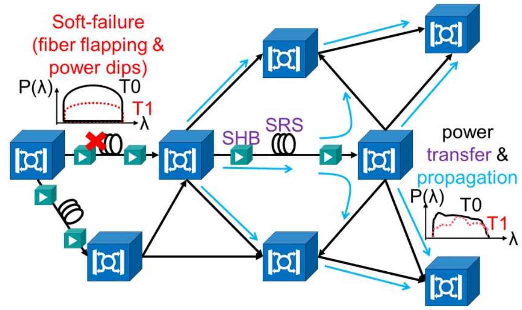

Fig. 1: Power dips and propagation in a mesh network.

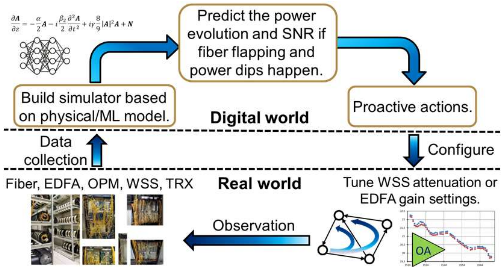

Fig. 2: DT work flow.

Algorithm 1 Loss margin based on DT risk map

Definition OMS_m: the mth OMS in the network, $SPAN_n$: the nth span in an OMS, $\varepsilon_{m,n,\delta}$: network SNR margin.
For OMS_m in $NETWORK$
  For $SPAN_n$ in OMS_m
    For δ in sweep range
      Add extra loss δ at input of $SPAN_n$
      Power propagation in DT
      Estimate $\varepsilon_{m,n,\delta}$
      If $\varepsilon_{m,n,\delta} \leq 0$ **then**
        Return loss margin δ_{margin}

accumulate between links and nodes. This cascading power transfer mechanism highlights the critical role of jointly considering SRS, SHB, and network topology when modeling and proactively mitigating impairment propagation [14]. These behaviors can be modeling based on machine learning (ML) model [15][14][16] and Gaussian noise (GN) model [17].

We propose a DT work flow (Fig. 2) with risk map algorithm (Alg. 1) to evaluate the robustness of a mesh network by systematically probing localized perturbations and observing their end-to-end impact. The algorithm iterates over each optical multiplex section (OMS_m) and, within it, each fiber span ($SPAN_n$). For every span, an extra loss δ is introduced at its input to emulate fiber flapping–induced power drops. Using the DT model, the resulting power propagation is evaluated to compute the corresponding network-wide SNR margin:

$$\varepsilon_{m,n,\delta} = \min_{\text{svc}}(SNR_{svc} - SNR_{FEC}) \quad (1)$$

which represents the minimum SNR margin across all services relative to the forward error correction (FEC) threshold.

By sweeping δ over a predefined range, the Alg. 1 identifies the critical threshold δ_{margin} as:

$$\delta_{margin} = \min\{\delta | \varepsilon_{m,n,\delta} \leq 0\} \quad (2)$$

at which service failure occurs. δ_{margin} is recorded as the risk indicator for $SPAN_n$, effectively mapping the network's vulnerability landscape and enabling proactive mitigation strategies.

Experimental Setup

The C-band network testbed, shown in Fig. 3, consists of six nodes interconnected in a mesh topology with 8 OMSs. Each OMS is composed of a pair of add/drop wavelength selective switches (WSSes), multiple fiber spans with various of types and lengths, and EDFAs operating in gain-lock mode with fixed gain and tilt settings. All optical power spectra are measured using commercial optical performance monitors (OPMs) installed at the outputs of booster amplifiers and pre-amplifiers.

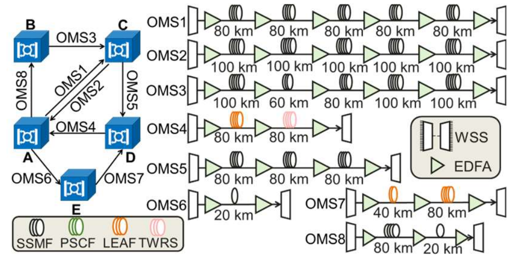

Fig. 3: Experimental setup.

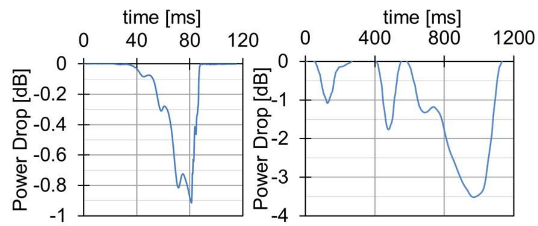

Fig. 4: Examples of power dips during fiber flapping.

A total of 40 services are emulated in the network using ASE loading with a 150 GHz channel spacing and measured by an 800 Gb/s 140GBaud PCS-16QAM real time transponder. Traffic is distributed among all node pairs, with two services established for each source–destination pair, spanning total transmission distances ranging from 20 km to 940 km. All services are provisioned following the set-and-forget strategy with flat power target and are established in a random order, resulting in a non-optimized initial power profile.

We emulated fiber flapping by manually shaking the fiber connector and recorded the power traces with a 0.2 ms–resolution power meter shown in Fig. 4, showing drops of several dB lasting ~40–400 ms. In the simulations, we normalize the dips by their maximum attenuation, then sweep the attenuation from 1dB to 6dB with 0.1dB interval for δ_{margin} calculation (Alg. 1). For experimental validations, we use variable optical attenuators (VOAs) to emulate the power dips.

Results

Visualization of Risk Maps

Fig. 5 illustrates the baseline risk map of fiber flapping at span input obtained after set-and-forget service provisioning. Each directed span is annotated with a colored arrow. The color of each

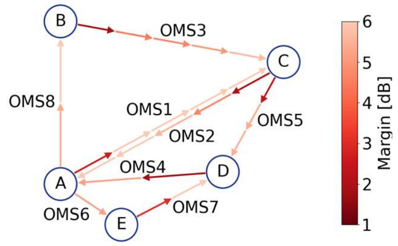

Fig. 5: Visualization of risk map (baseline).

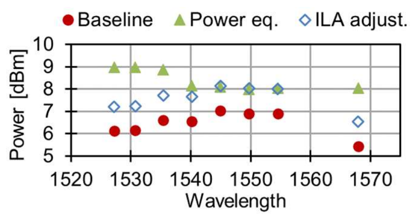

Fig. 6: Power spectra at output of the 1st ILA of OMS3.

arrow encodes the fiber input loss margin which represents the network SNR margin degradation sensitivity when an extra-loss at fiber input connector is hypothetically introduced on that specific span. In other words, for each span, the DT evaluates how much extra loss at span input can be tolerated before the SNR margin reaches zero. In the baseline scenario, deep-red spans mark weak points highly sensitive to fiber flapping, causing power dips and network-wide SNR margin degradation.

Proactive Management

First of all, we apply power equalization on our setup (we estimate ASE and nonlinear noises per service per OMS P_{ASE}, P_{NLI} with the DT and compute the service launch powers such that $P_{ASE}=2P_{NLI}$ [18]) after 40 services are established. For example, the power spectra at ouput of an ILA before and after adjustments are shown in Fig. 6. As a result, the risk map becomes significantly more uniform, with most spans transitioning to the low-risk region (Fig. 7).

Besides, we observe that power drops occurring in the first span have the most pronounced impact on system-level performance, as impairments introduced at this early stage propagate and accumulate along the light path. Therefore, in addition to global power equalization, we further consider pre-compensation by adjusting the inline amplifier (ILA) to mitigate potential risks. To this end, we pro-actively boost the gain of the ILAs located on the risky spans by 1dB, which may slightly degrade the SNR of some services, but make those services more tolerant to fiber flapping. The new risk map is shown in Fig. 8.

Compared with the baseline (Fig. 5), the ILA adjustment strategy (Fig. 8) reduces risk over a wider range of spans, whereas the power equalization strategy (Fig. 7) achieves a more pronounced risk reduction across the majority of spans. Overall, these strategies demonstrate a

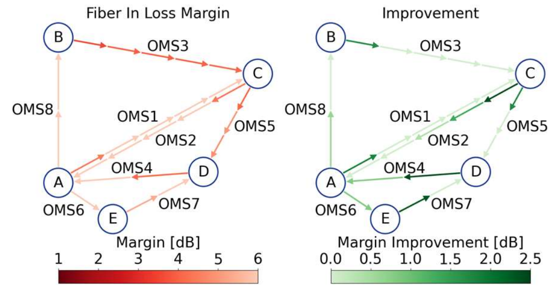

Fig. 7: Risk maps after power equalization.

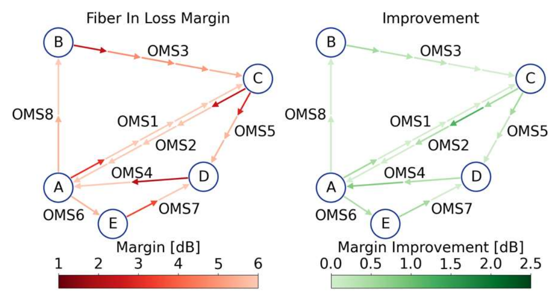

Fig. 8: Risk maps after 1dB pre-compensation of first ILA.

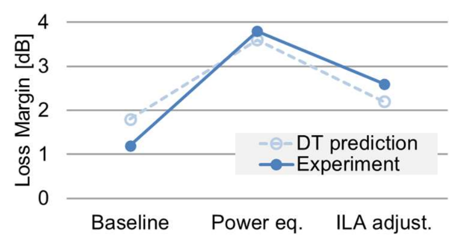

Fig. 9: Margin improvement with proactive adjustments.

favorable trade-off between performance improvement and operational complexity, thereby validating the effectiveness of risk-map-driven proactive management of fiber flapping.

Finally, Fig. 9 summarizes the lowest loss margin in the network introduced by fiber flapping in difference cases. Power equalization yields the largest improvement, increasing the loss margin by 2.6dB in experimental measurements. The ILA 1dB-pre-compensation scheme provides a 1.4dB enhancement, albeit to a lesser extent, validating that even lightweight, proactive adjustments can substantially improve loss margin. These results highlight the capability of the proposed DT-based risk map to identify critical spans and guide efficient mitigation strategies.

Conclusions

We implement and evaluate a proactive management strategy based on DT risk maps to improve end-to-end SNR margin with fiber flapping on a mesh network testbed. The experimental results demonstrate that the proposed framework can enhance network resilience under uncertain short-term link intermittency conditions and provide an experimental pathway for future autonomous optical networks operating under low-margin conditions.

References

[1] C. Delezoide, P. Ramantanis and P. Layec, "Investigating Q-drops and Their Probable Causes," *2022 European Conference on Optical Communication (ECOC)*, Basel, Switzerland, 2022, pp. 1-4.

[2] S. Li, Y. Song, Z. Cui, J. Li, M. Zhang, and D. Wang, "Simple and Fast Optical Fiber Flap Localization Based on Two-Edge Channel Power in Wideband System," *2025 Optical Fiber Communications Conference and Exhibition (OFC)*, San Francisco, CA, USA, 2025, pp. 1-3.

[3] R. Forbes, L. Licciardi, Y. Nakajima, N. Sampson, F. Naim, B. Radier, A. Artigiani, O. Ferveur, M. Brunner, Y. Xie, F. Camacho, and Y. Zeng, "ETSI White Paper No. 69: AI in the evolution of Autonomous Networks—ETSI perspectives and major achievements," White Paper, First edition, Nov. 2025. [Online].

[4] C. Janz, Y. You, M. Hemmati, A. Javadtalab, Z. Jiang, H. Li, and H. Feng, "Invited paper: Network digital twins for optical networks," *Optical Fiber Technology*, vol. 89, no. 104068, 2025, DOI: 10.1016/j.yofte.2024.104068

[5] D. Wang, Y. Song, Y. Zhang, X. Jiang, J. Dong, F. N. Khan, T. Sasai, S. Huang, A. P. T. Lau, M. Tornatore, and M. Zhang, "Digital Twin of Optical Networks: A Review of Recent Advances and Future Trends," *Journal of Lightwave Technology*, vol. 42, no. 12, p.p. 4233–4259, 2024, DOI: 10.1109/JLT.2024.3401419

[6] Q. Zhuge, X. Liu, Y. Zhang, M. Cai, Y. Liu, Q. Qiu, X. Zhong, J. Wu, R. Gao, L. Yi, and W. Hu, "Building a digital twin for intelligent optical networks [Invited Tutorial]," *Journal of Optical Communications and Networking*, vol. 15, C242–C262, 2023, DOI: 10.1364/JOCN.483600

[7] R. Vilalta, L. Gifre, R. Casellas, R. Muñoz, R. Martínez, A. Mozo, A. Pastor, D. López, and J. P. Fernández-Palacios, "Applying Digital Twins to Optical Networks with Cloud-Native SDN Controllers," *IEEE Communications Magazine*, vol. 61, p.p. 128–134, 2023, DOI: 10.1109/MCOM.003.2300105

[8] M. S. Faruk and S. J. Savory, "Measurement Informed Models and Digital Twins for Optical Fiber Communication Systems," *Journal of Lightwave Technology*, vol. 42, no. 3, p.p. 1016–1030, 2024, DOI: 10.1109/JLT.2023.3328765

[9] C. Sun, X. Yang, G. Charlet, P. A. Stavrou, and Y. Pointurier, "Digital twin-enabled multi-step strategies for autonomous power equalization in optical networks," *Journal of Optical Communications and Networking*, vol. 17, no. 7, p.p. C41-C50, 2025, DOI: 10.1364/JOCN.549934

[10] K. Christodoulopoulos, C. Delezoide, N. Sambo, A. Kretsis, I. Sartzetakis, A. Sgambelluri, N. Argyris, G. Kanakis, P. Giardina, G. Bernini, D. Roccato, A. Percelsi, R. Morro, H. Avramopoulos, P. Castoldi, P. Layec, and S. Bigo, "Toward efficient, reliable, and autonomous optical networks: the ORCHESTRA solution [Invited]," *Journal of Optical Communications and Networking*, vol. 11, no. 9, pp. C10-C24, 2019, DOI: 10.1364/JOCN.11.000C10

[11] D. Wang, Z. Zhang, M. Zhang, M. Fu, J. Li, S. Cai, C. Zhang, and X. Chen, "The role of digital twin in optical communication: Fault management, hardware configuration, and transmission simulation," *IEEE Communications Magazine*, vol. 59, no. 1, pp. 133–139, 2021, DOI: 10.1109/MCOM.001.2000727

[12] J.-P. Elbers and C. Fürst, "Chapter 7 - Spectral Power Fluctuations in DWDM Networks Caused by Spectral-Hole Burning and Stimulated Raman Scattering," *Optically Amplified WDM Networks* (J. Zyskind and A. Srivastava, eds.), pp. 201–219, Oxford: Academic Press, 2011, DOI: 10.1016/B978-0-12-374965-9.10007-X

[13] J. Junio, D. C. Kilper and V. W. S. Chan, "Channel power excursions from single-step channel provisioning," *Journal of Optical Communications and Networking*, vol. 4, no. 9, pp. A1-A7, 2012, DOI: 10.1364/JOCN.4.0000A1

[14] S. J. Savory, R. J. Vincent, and D. J. Ives, "Design considerations for low-margin elastic optical networks in the nonlinear regime [Invited]," *Journal of Optical Communications and Networking*, vol. 11, no. 10, pp. C76-C85, 2019, DOI: 10.1364/JOCN.11.000C76

[15] Z. Wang, D. C. Kilper and T. Chen, "Open EDFA gain spectrum dataset and its applications in data-driven EDFA gain modeling," *Journal of Optical Communications and Networking*, vol. 15, no. 9, pp. 588-599, 2023, DOI: 10.1364/JOCN.491901

[16] X. Jiang, J. Dong, Y. Song, J. Li, M. Zhang and D. Wang, "Physics-Informed Machine Learning for EDFA: Parameter Identification and Gain Estimation," *Journal of Lightwave Technology*, vol. 43, no. 11, pp. 5040-5054, 2025, DOI: 10.1109/JLT.2025.3548285

[17] D. Semrau, R. I. Killey and P. Bayvel, "A Closed-Form Approximation of the Gaussian Noise Model in the Presence of Inter-Channel Stimulated Raman Scattering," *Journal of Lightwave Technology*, vol. 37, no. 9, pp. 1924-1936, 2019, DOI: 10.1109/JLT.2019.2895237

[18] P. Poggiolini, G. Bosco, A. Carena, V. Curri, Y. Jiang, and F. Forghieri, "The GN-Model of Fiber Non-Linear Propagation and its Applications," *Journal of Lightwave Technology*, vol. 32, no. 4, p.p. 694-721, Feb. 2014, DOI: JLT.2013.2295208